

1 **Influence of Nozzle Diameter on the Anisotropy of Compressive**
2 **Strength – Measured on 3D Printing Concrete Designed with**
3 **Recycled Fine Aggregates**

4 Yeakleang Mui¹, Luc Courard¹, David Bulteel^{2,3}, Sébastien Rémond⁴, Maria Taleb^{2,3},
5 Khadija El Cheikh⁵ and Julien Hubert¹

6 ¹University of Liege, Urban and Environmental Engineering, Building Materials, Quartier Polytech
7 1, Allée de la découverte 9, B-4000 Liège, Belgium

8 ²IMT Nord Europe, Institut Mines-Telecom, centre of Materials and Processes, F-59000 Lille,
9 France

10 ³Univ. Lille, Institut Mines-Télécom, Univ. Artois, Junia, ULR 4515 - LGCgE – Laboratoire de
11 Génie Civil et géoEnvironnement, F-59000 Lille, France

12 ⁴Univ Orléans, Univ Tours, INSA CVL, LaMé, EA 7494, Rue Léonard De Vinci, 45072 Orléans,
13 France

14 ⁵Concrete Technology Laboratory, Buildwise, Avenue P. Holoffe 21, 1342 Limelette, Belgium
15 yeakleang.muy@uliege.be

16 **Abstract.** 3D printing concrete (3DPC) is an innovative method in the construction sector,
17 eliminating the need for traditional formwork. This study introduces a mortar mixed design
18 with recycled fine aggregates (RFA) where $d_{\max} < 2$ mm. The mortar was printed with two
19 different printers, each equipped with nozzles of different diameters (2 cm and 4 cm). The
20 layers were printed and pressed to widen the string to the chosen width of 6 cm. The primary
21 objective is to study the influence of nozzle diameters on the mechanical properties as well
22 as the anisotropic behavior of 3DPC. The investigation was conducted through mechanical
23 testing on different orientations of printed layers, parallel (oz) and perpendicular (ox) to the
24 printing direction. Results reveal a significant drop of compressive strength in the orientation
25 (oz) when using a 2 cm nozzle compared to a 4 cm nozzle from the same mix design. This
26 is attributed to the intense compression of each layer during deposition to ensure controlled
27 spreading of the material path consequently creating damage in the outer parts of the printed
28 concrete.

Keywords: 3D printing concrete; Nozzle dimension, Anisotropy compressive strength,
Interlayer bond strength

29 **1 Introduction**

30 In recent years, the construction industry has witnessed the development of a new building
31 technology driven by innovations in additive manufacturing technologies, commonly
32 referred to as 3D printing (3DP). This technique is considered a cornerstone of industrial
33 4.0. Three-dimensional printing is an innovative technique that entails the sequential
34 deposition of layers, pioneered in 1986 by C. Hull for prototyping purposes [1]. Compared
35 with traditional concrete (cast-in-situ), 3DPC presents several advantages such as the
36 freedom of design, formwork-free fabrication, waste minimization and mass customization
37 [1-2].

38 3D printing concrete (3DPC) is being explored as part of the construction industry's shift
39 towards more sustainable and eco-friendly building solutions. While the technology offers
40 improved material efficiency [3-4], challenges persist due to the significant use of cement
41 and sand [4]. To address this, incorporating recycled materials into 3DPC formulations
42 shows promise for reducing environmental impact and promoting a circular economy.

43 In addition to mix design, printing parameters such as nozzle geometry [5], nozzle distancing
44 [6-7], printing speed [7-8], and printing time-gap [9] also influence the performance of
45 printed concrete, particularly the interlayer bond strength, which may lead to issues such as
46 "cold joint" [10].

47 Despite extensive research on various parameters affecting the mechanical strength of
48 3DPC, the influence of nozzle diameter on mechanical strength has not been addressed
49 elsewhere. This paper investigates this issue, including an examination of the failure patterns
50 of interlayer bond strength using direct tensile testing.

51 **2 MATERIALS AND METHODS**

52 **2.1 Materials**

53 The recycled aggregate from the recycling of all-mixture concrete, denoted as recycled sand
54 (RS), originates from the Tradecowall recycling center in St-Ghislain, Belgium. This RS
55 possesses a maximum grain size of 2 mm with a density of 2.39 tons/m³ and exhibits a water
56 absorption rate of 5.31%. The cement employed in this mix is categorized as type CEMI
57 52.5N with a density of 3.16 tons/m³, procured from VICAT's manufacturing facility in
58 Créchy, France. The plasticizer Polycarboxylate (PCE) and the viscosity modifying
59 admixture (VMA) used in this research were supplied by Chryso company.

60 2.2 Mixture proportion and sample implementation

61 For the mix preparation, the composition is listed in Table 1 and the mixing procedure is
 62 initiated by mixing the first third of the materials, including sand, cement, and water, for a
 63 period of 2 min. This is followed by the inclusion of the second portion, in which the
 64 admixtures are added to the water, which is similarly mixed for 2 min. Lastly, the third
 65 portion is introduced and blended for an additional 11 min.

66 Table 1- Mixtures proportions of mortars (kg)

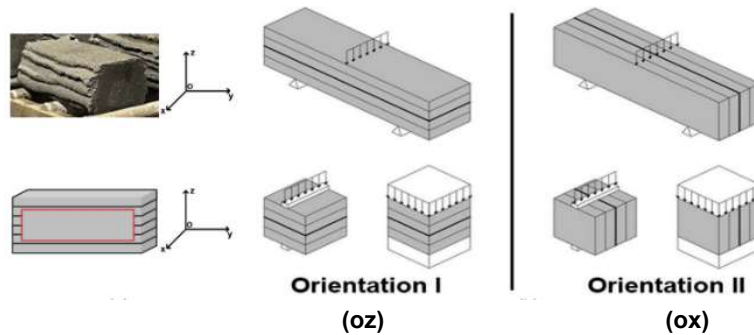
	Cement	Sand	Water	Plasticizer	VCA	W_{eff}/C
RSM/NSM	905,00	995,60	313,52	22,63	1,81	0,29

67 Specifically, "S"-shaped elements were continuously printed up to 6 layers with a printing
 68 speed of 100 mm/s. Subsequently, these elements were covered with plastic film and left for
 69 24 h before being cured in a humid chamber (maintained at a relative humidity of $95\pm 5\%$
 70 and a temperature of $20\pm 2^\circ\text{C}$).

71 2.3 EXPERIMENTAL METHODS

72 **Compressive strength test.** Compressive strength R_c evaluations were executed following
 73 the protocols outlined in the established standard NBN EN 196-1 [11]. Test prisms with
 74 dimensions of $40 \times 40 \times 160 \text{ mm}^3$ were sawed from the "S" shaped elements and tested at
 75 intervals of 28, 56, and 91 days for samples printed with a 2 cm nozzle and exclusively at
 76 28 days for samples printed with a 4 cm nozzle.

77 All extracted samples at each designated time were tested following two distinctive loading
 78 directions: (ox) and (oz), as shown in Figure 1.

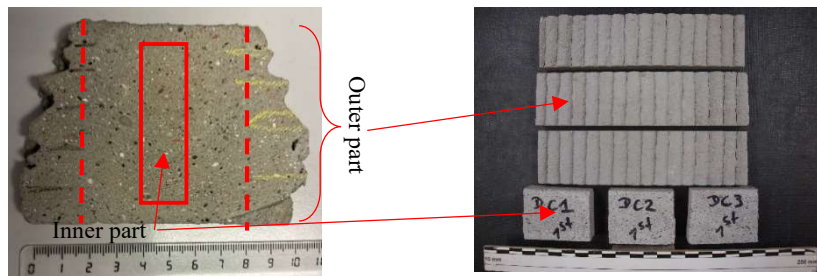


79 Figure 1- Printing samples and orientations of loading direction [12-13]

80 **Direct Tensile test.** Tensile strength R_t was evaluated following the guidelines outlined in
 81 the established standard NBN B15-211 [14]. Cylindrical specimens, measuring 50 mm in
 82 diameter and 50 mm in height, were drilled from the S shaped elements and tested at
 83 intervals of 28, 56, and 91 days for cast samples and exclusively at 91 days for printed
 84 samples. All samples were vertically drilled perpendicularly to the printed layers from the
 85 printed “S” shape element. The outline of the layers was then traced approximately based
 86 on the visible interface on the printed element. The experimental procedure was executed
 87 using an INSTRON instrument with a pulling rate set at 0.10 ± 0.05 MPa/s.

88 **Porosity and bulk density measurements.** Porosity ε and bulk density ρ_d of the mortar
 89 were evaluated following standard NF P18-459 [15]. Cube-shaped samples extracted from
 90 the printed “S” element, measuring $40 \times 40 \times 40$ mm³, were employed for these
 91 measurements, and both cases of sample printing with 2 cm and 4 cm nozzle. The assessment
 92 was conducted at specific time intervals: 28 and 56 days.

93 For the microstructural comprehension, a complementary investigation was conducted on
 94 the inner and the outer parts of the printed sample, as shown in Figure 2 resulting from the
 95 printing with 2 cm and 4 cm nozzle at 270 days and 210 days of curing respectively.



96 Figure 2- Sample preparation for complementary results for the porosity test

97 3 RESULTS AND DISCUSSION

98 3.1 Effect nozzle diameter on the anisotropy of compressive strength of mortar

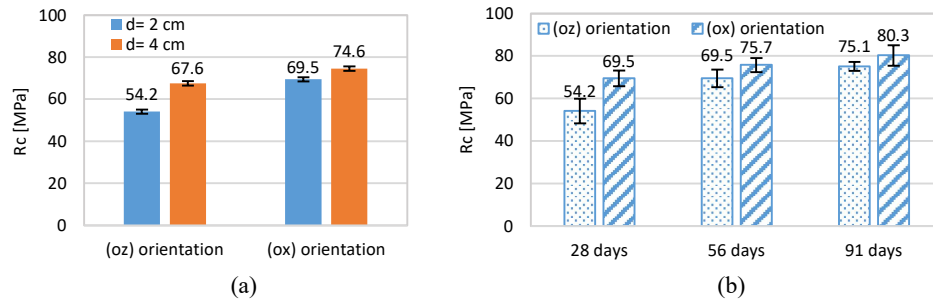
99 Figure 3 illustrates the printed bench within the context of the CIRMAP research project
 100 [16]. This achievement was accomplished by printing the bench in multiple segments and
 101 assembling them afterward. Consequently, each segment exhibits a non-planar
 102 configuration, requiring the nozzle to move to different levels during printing, ultimately
 103 resulting in the pushing down of the filament.



104
105

Figure 3- Printed segment assembled as a bench in the framework of CIRMAP project [16]

106 Figure 4(a) depicts the compressive strength at 28 days of printed samples using 2 cm and 4
107 cm nozzle diameters. When applying load in the (oz) orientation, a significant reduction in
108 R_c of approximately 19.8% was observed, decreasing from 67.6 MPa to 54.2 MPa when
109 using a 4 cm and 2 cm nozzle respectively. The samples produced with a 2 cm nozzle
110 diameter tend to exhibit a weak lateral surface (outer part, as shown in Figure 2), which
111 contributes to lower compressive strength in the direction (ox) compared to (oy), as indicated
112 by the satisfactory theoretical failures of the cube's compressive strength [17]. The action
113 of pushing down the string to achieve a 6 cm string width resulted in damage to the lateral
114 printing surface, ultimately leading to dehydration of the lateral surface and simultaneously
115 limiting the hydration of cement. However, after sufficient curing in the chamber with
116 relative humidity (HR) greater than 95%, the compressive strength (R_c) tends to significantly
117 increase due to the development of cement hydration, as depicted in Figure 4(b). These
118 results reflect the mechanical behavior of the actual printed element shown in Figure 3.



119 Figure 4- R_c of the printed sample with a 2 cm and a 4 cm nozzle at 28 days (a) and R_c of the printed
120 sample using a 2 cm nozzle at 28, 56, and 91 days

121 3.2 Effect nozzle diameter on the microstructure of mortar

122 Table 2 presents the results of the porosity and bulk density of printed samples using a 2 cm
123 nozzle and a 4 cm nozzle at 28 and 56 days. Overall, the porosity of the printed samples
124 using a 2 cm nozzle is higher than those using a 4 cm nozzle, with a difference of 0.7% and
125 1.4% at 28 days and 56 days respectively. This higher porosity is primarily caused by the
126 level of damage to the lateral surface, as described in Section 2.3. This damage results in
127 excessive drying of the lateral surfaces and may potentially disrupt hydration. Additionally,
128 the difference between the porosity of the outer and inner parts is generally greater for

129 samples printed using a 2 cm nozzle compared to those printed using a 4 cm nozzle, as
 130 illustrated in Table 3. Unlike porosity, there is no remarkable change in bulk density between
 131 the inner and outer parts of the printed sample.

132 Table 2- Porosity and bulk density of printed sample using a 2 cm nozzle and a 4 cm nozzle at 28
 133 and 56 days

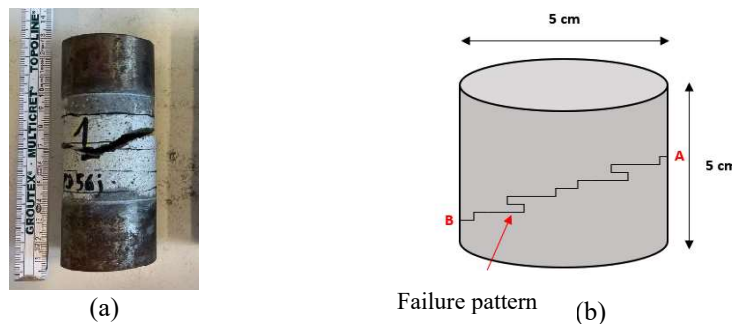
	d= 2 cm		d= 4 cm	
	Porosity [%]	Bulk density [kg/m ³]	Porosity [%]	Bulk density [kg/m ³]
28 days	18.3 ± 0.4	2003	17.6 ± 0.4	2002
56 days	18.2 ± 0.1	2004	15.8 ± 0.1	2014

134 Table 3- Porosity and bulk density of inner part and outer part of the printed sample using a 2 cm
 135 nozzle and a 4 cm nozzle

	d= 2 cm at 270 days		d= 4 cm at 210 days	
	Porosity [%]	Bulk density [kg/m ³]	Porosity [%]	Bulk density [kg/m ³]
Inner part	17.8 ± 0.2	2045	17.2 ± 0.1	2024
Outer part	18.5 ± 0.2	2018	17.7 ± 0.4	2032

136 3.3 Bonding properties between layers of printed mortar

137 The direct tensile strength (Rt) at 28, 56, and 91 days of the samples printed with a 2 cm
 138 nozzle are 2.51, 2.69, and 2.25 MPa respectively. The investigation focused on the failure
 139 pattern of direct tensile strength. As depicted in Figure 2, there was no visible trace observed
 140 between layers on the vertical cutting surface. This absence can be attributed to the minimal
 141 time gap allocated for printing each layer (50 s per layer). A similar result was reported in
 142 the research conducted by Tay et al. [9]. The minimal time gap between layers does not
 143 allow the interlayer surface to form a cold joint. Consequently, the failure pattern does not
 144 exhibit weakness between the layers, as the failure originates diagonally, as depicted in
 145 Figure 5.



146 Figure 5- Failure pattern of printed specimens after tensile test

147 4 CONCLUSION

148 This research study has illuminated various critical aspects related to 3D-printed mortar,
149 particularly focusing on the impact of using different nozzle sizes on the mechanical
150 behavior and microstructure of mortar containing 100% Recycled Fine Aggregates (RFA).
151 The conclusions can be summarized as follows:

- 152 ▪ A minimum compressive strength of 54.2 MPa was achieved with 100% RFA at
153 28 days.
- 154 ▪ Anisotropy in compressive strength was observed, with greater strength when
155 compressing the sample perpendicularly to the layer's deposition. This strength was
156 found to be 19.8% higher compared to compression parallel to the layer deposition.
- 157 ▪ Using a 2 cm nozzle diameter created a weaker lateral surface (outer part) compared
158 to that when using a 4 cm nozzle diameter. The smaller the nozzle diameter, the
159 greater damage was observed. It is recommended to use a nozzle diameter as close
160 as possible to the desired string width to avoid the need for widening it by
161 compressing the layers together. This pressure tends to damage the lateral surface
162 which compromises the structural stability of the entire string.
- 163 ▪ The porosity of the samples printed with a 2 cm nozzle diameter is 0.7% and 1.4%
164 higher than that of the samples printed with a 4 cm nozzle diameter at 28 and 56
165 days respectively.
- 166 ▪ The porosity of the outer part of the printed sample is typically higher than that of
167 the inner part. Specifically, the difference in porosity between the inner and outer
168 parts was observed to be 0.7% when utilizing a 2 cm nozzle diameter and 0.5%
169 when employing a 4 cm nozzle diameter.
- 170 ▪ Given the minimal time gap, the failure of tensile strength is not affected by the
171 interface between layers, as the rupture occurs randomly. These findings challenge
172 traditional assumptions regarding the existence of a weaker interface between
173 layers of 3D-printed materials and underscore the need for further research.

174 These results highlight additional parameters that may influence the performance of 3DPC,
175 in addition to those identified in previous research. However, further research is needed to
176 ensure the statistical accuracy of these results.

177 ACKNOWLEDGEMENT

178 The authors extend their gratitude to the Interreg North-West Europe program for providing
179 funding for this research within the framework of the CIRMAP project.

180

REFERENCES

- 181 [1] C. W. Hull, "Apparatus for production of three-dimensional objects by stereolithography,"
182 US4575330A, Mar. 11, 1986
- 183 [2] T. D. Ngo, A. Kashani, G. Imbalzano, K. T. Q. Nguyen, and D. Hui, "Additive manufacturing
184 (3D printing): A review of materials, methods, applications and challenges," *Composites Part B:
185 Engineering*, vol. 143, pp. 172–196, Jun. 2018.
- 186 [3] B. L. Damineli, F. M. Kemeid, P. S. Aguiar, and V. M. John, "Measuring the eco-efficiency of
187 cement use," *Cement and Concrete Composites*, vol. 32, no. 8, pp. 555–562, Sep. 2010.
- 188 [4] C. Zhang *et al.*, "Mix design concepts for 3D printable concrete: A review," *Cement and
189 Concrete Composites*, vol. 122, p. 104155, Sep. 2021.
- 190 [5] G. Ji, J. Xiao, P. Zhi, Y.-C. Wu, and N. Han, "Effects of extrusion parameters on properties of
191 3D printing concrete with coarse aggregates," *Construction and Building Materials*, vol. 325, p.
192 126740, Mar. 2022.
- 193 [6] V. N. Nerella, S. Hempel, and V. Mechtcherine, "Effects of layer-interface properties on
194 mechanical performance of concrete elements produced by extrusion-based 3D-printing,"
195 *Construction and Building Materials*, vol. 205, pp. 586–601, Apr. 2019.
- 196 [7] B. Panda, S. C. Paul, N. A. N. Mohamed, Y. W. D. Tay, and M. J. Tan, "Measurement of tensile
197 bond strength of 3D printed geopolymers mortar," *Measurement*, vol. 113, pp. 108–116, Jan.
198 2018.
- 199 [8] J. Van Der Putten, G. De Schutter, and K. Tittelboom, "The Effect of Print Parameters on the
200 (Micro)structure of 3D Printed Cementitious Materials," in *RILEM Bookseries*, 2019, pp. 234–
201 244.
- 202 [9] Y. W. D. Tay, G. H. A. Ting, Y. Qian, B. Panda, L. He, and M. J. Tan, "Time gap effect on bond
203 strength of 3D-printed concrete," *Virtual and Physical Prototyping*, vol. 14, no. 1, pp. 104–113,
204 Jan. 2019.
- 205 [10] S. Kosmatka, B. Kerkhoff, and W. Panarese, *Design and Control of Concrete Mixtures*. 2002.
- 206 [11] NBN EN 196-1, "Méthode d'essais des ciments - Partie 1: Détermination des résistances." 2016.
- 207 [12] Y. Muy *et al.*, "INFLUENCE DE L'UTILISATION DE GRANULATS FINS RECYCLES SUR
208 LES PROPRIETES MECANIQUE DES BETONS IMPRIME 3D".
- 209 [13] R. J. M. Wolfs, F. P. Bos, and T. A. M. Salet, "Hardened properties of 3D printed concrete: The
210 influence of process parameters on interlayer adhesion," *Cement and Concrete Research*, vol.
211 119, pp. 132–140, May 2019.
- 212 [14] NBN B 15 211, "Concrete testing - Direct tensile strength." 1974.
- 213 [15] NF P18-459, "Essai pour béton durci - Essai de porosité et de masse volumique," p. 9p, Mar.
214 2010.
- 215 [16] CIRMAP, "Circular economy via customisable furniture with Recycled Materials for public
216 Places | Interreg NWE."
- 217 [17] NBN EN 12390-3, "Essais pour béton durci - Partie 3: Résistance à la compression des
218 éprouvettes," 2019.
- 219